JOURNAL OF MATERIALS SCIENCE **35** (2000) 1917–1924

Transient liquid phase bonding process using liquid phase sintered alloy as an interlayer material

Y.-S. KWON, J.-S. KIM, J.-S. MOON
RRC Research Center for Machine Parts & Materials Processing and School of Materials and Metallurgical Engineering, University of Ulsan, Ulsan 680-749, South Korea

M.-J. SUK*
Department of Metallurgical Engineering, Samchok National University, Samchok 245-711, South Korea
E-mail: panpani@samchok.ac.kr

An attempt was made of using a liquid phase sintered alloy, which will be a liquid phase coexisting with solid particles at the bonding temperature, as an interlayer for bonding metals. With an aim of revealing the fundamental features of this modified TLP bonding, investigated were the kinetics concerned with the isothermal solidification process and the growth of solid particles in Fe-4.5wt%P and Fe-1.16wt%B interlayers for bonding pure iron. The movement of the bond interface was linearly dependent on $t^{1/2}$ with higher slope than expected in the normal TLP bonding. The higher slope is attributed to the contribution of the solid particles distributed in the interlayer. The solid particles have shown no growth. However, when pure Fe particles are allowed to coexist with the liquid of equilibrium composition, they grows very rapidly. Discussion was made on the growth kinetics of the pure Fe particles.

1. Introduction

Transient liquid phase (TLP) bonding is a metal joining process which has critical advantages other joining processes could not provide. A thin interlayer alloy containing elements for depressing melting point is inserted as a bonding agent between the base metals. At the bonding temperature the interlayer temporarily melts filling the gaps between the mating surfaces, and subsequently isothermal solidification occurs by interdiffusion of the depressant element, thereby forming a bond while at that temperature.

Since its first development and application for joining Ni-base superalloys [1], the TLP bonding process has shown broad applicability covering almost all kinds of heat resistant alloys, especially in the alloy systems which are prone to either hot cracking during fusion welding or losing the inherent mechanical properties when employing the joining method other than TLP bonding.

In the conventional TLP bonding described above, the interlayer alloy inserted is fully liquid at the bonding temperature. If, instead of forming fully liquid phase, a definite fraction of solid phase is allowed to be present at the bonding temperature, the time required for isothermal solidification of interlayer alloy will be reduced, although the major time consuming step in the TLP bonding process will be homogenization step continued after the isothermal solidification. Recently, even the homogenization step was reported to be shortened by adding the metal powders to the interlayer [2]. On the other hand, in case of large bonding clearance which amounts to several hundreds μm it will be also possible to complete isothermal solidification within a reasonable time. However, in conventional TLP bonding this is impossible or a lot of time is required. In the present work an attempt was made of using a liquid phase sintered alloy as an interlayer material, where the solid and liquid phases would coexist at the bonding temperature. With an aim of revealing the fundamental features of this modified TLP bonding, investigated were the kinetics concerned with the isothermal solidification process (that is, inward movement of the bonding interface between the base metal and the interlayer) and the growth of solid particles.

2. Experimental procedure

Hot rolled pure iron plate (99.98% purity) was used for base metal which has a dimension of $10 \times 10 \times 5$ (mm), while Fe-4.5wt%P and Fe-1.16wt%B alloys which had been previously sintered were employed as an interlayer material. The sintered interlayer materials were prepared from carbonyl Fe powder with a mean particle size of 44 μm, prealloyed Fe-18.4wt%B powder

* Author to whom all correspondence should be addressed.

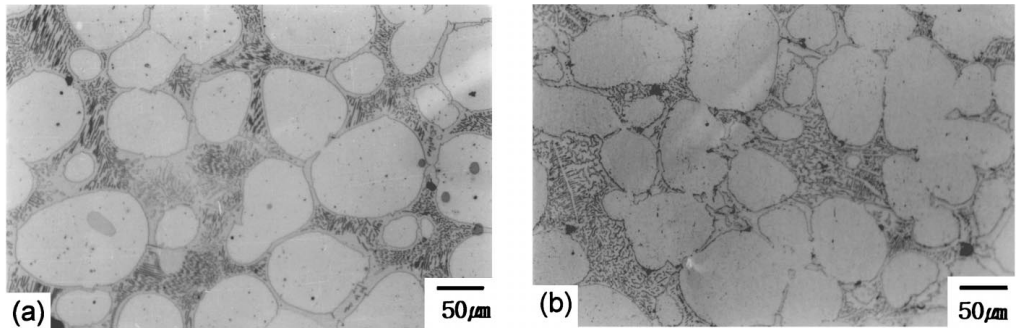

Figure 1 Microstructures of the liquid phase sintetred alloys (sintering time: 3.6×10^3 s). (a) Fe-4.5wt%P sintered at 1473 K, (b) Fe-1.16wt%B sintered at 1523 K.

of -325 mesh and Fe_2P powder of $-325 + 400$ mesh. Sintering was conducted in H_2 for 3.6×10^3 s at 1473 K and 1523 K for Fe-4.5wt%P and Fe-1.16wt%B alloys, respectively. Fig. 1 shows the sintered microstructures in which the volume fractions of the solid are 0.67 and 0.62 for Fe-4.5wt%P and Fe-1.16wt%B, respectively. The sintered alloys were then sliced to 500 μm in thickness, and the base metals as well as the interlayer alloys were mechanically polished in order to ensure flatness of the surface and the desired width. The bonding treatment was carried out at the same temperature as sintering in induction heating chamber which is evacuated to about 4×10^{-3} Pa. In order to prevent from flooding of the liquid phase of the interlayer and to maintain the desired spacing, platinum spacer with a diameter of 500 μm was put into between both mating surfaces. In the induction heating chamber very rapid heating and cooling were established, the heating and cooling rates being 4.5 and 5 K/s, respectively, and thus an additional heat effect during heating and cooling which otherwise might be serious can be minimized.

The travel distance of the bond interface, X, was evaluated from $\frac{500 - W}{2}$ where W is the width of interlayer in μm. The width of the interlayer was measured at 150 μm interval along the entire bond interface, with approximately 60 readings taken. Mean particle size was obtained employing linear intercept method [3]. An experiment was also carried out in which pure Fe powders are allowed to coexist with a liquid of equilibrium concentration in the interlayer. For this purpose the pure Fe powders were stacked between the base metals on a sheet of Fe-P or Fe-B alloys which had been previously prepared to have equilibrium liquidus compositions at the bonding temperatures, i.e. Fe-7.8wt%P and Fe-3.2wt%B. In this case the width of the interlayer was initially held 1 mm to permit enough space for the probable particle growth, and Al_2O_3 spacer with 1 mm thickness was employed to initially maintain the desired width of the interlayer.

3. Results

The bond interface between the base metal and the interlayer moves inward from the original position with increasing bond treatment time, as shown in Fig. 2. The bond treatment temperature and the sintering temperature are the same, being 1473 K for

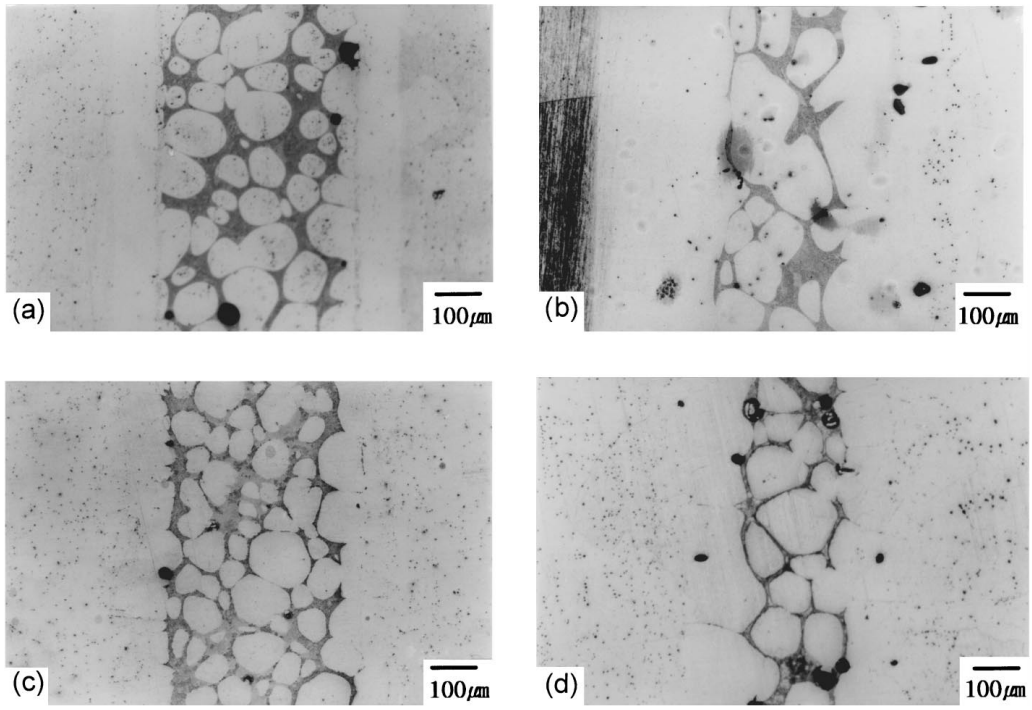

Figure 2 The microstructure of interlayer during TLP bonding of pure Iron. The interlayer alloys and the bonding temperatures are (a, b) Fe-4.5wt%P, 1473 K and (c, d) Fe-1.16wt%B, 1523 K. (a, c) 600 s, (b, d) 3600 s.

Fe-4.5wt%P interlayer and 1523 K for Fe-1.16wt%B interlayer. Whereas in conventional TLP bonding process dissolution of base metal into the liquid interlayer usually occurs, the TLP bonding using liquid phase sintered interlayer undergoes no melting of base metal because the equilibrium concentration of the liquid phase is already attained in the as-sintered state. The travel distance of the bond interface, X, can be expressed by the following equation [4–6].

$$X = K(Dt)^{1/2} \tag{1}$$

where K is constant, D solute diffusion coefficient, and t time.

The experimental results shown in Fig. 3 also indicates the similar trend to the Equation 1, the distance linearly depending on $t^{1/2}$. The result shows a definite movement of the bond interface even at $t = 0$. This is because some of the solid particles randomly distributed are attached to the interface during heating up to the bond temperature, constituting a part of base metal. The scatter bar of the data points represents standard deviation of the variation of the travel distance at different positions.

Fig. 4 shows a relationship between the particle size and the treatment time. The particle size remains nearly constant during the bond treatment up to 3.6×10^3 s. This implies that the growth of particle by Ostwald ripening [7] did not take place in the liquid pool of the interlayer even though there is a definite particle size distribution. As long as the interlayer plays a role as a solute source with respect to the mating base metal, there will be probably no chance for the solute atoms to be carried into or out of the particles concerned. The solute atom flux between the growing particle and the shrinking one will be overwhelmed by the flux macroscopically directed toward the base metal. However, when the particles are not in equilibrium with the liquid phase, they undergoes relatively rapid growth, although the growth rate sharply decreases after a certain time. Figs 5 and 6 show the growth of the solid particles in the interlayer. Here, pure Fe particles were inserted as an interlayer material together with Fe-7.8wt%P and Fe-3.2wt%B alloys, the compositions of which correspond to the equilibrium liquidus at the respective bonding temperatures. The interlayer then becomes a liquid of liquidus composition embedded by pure Fe particles at the bonding temperature, and the composition of the liquid will not be changed throughout the bonding treatment. It is unlikely that the growth proceeds at the expense of smaller particles. Rather, it is plausible to consider the particle growth as a similar process to the movement of the bond interface. Of course, this growth will be mitigated as the mean composition of the solid particles approaches the equilibrium value.

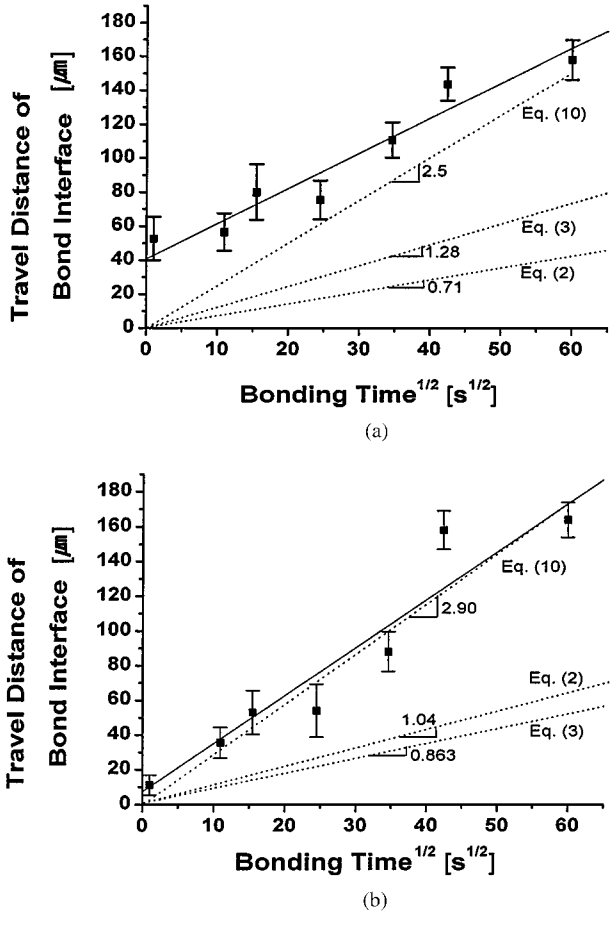

Figure 3 Relationship between the travel distance of the bond interface and the bonding time. The interlayer alloys are (a) Fe-4.5 wt%P, and (b) Fe-1.16wt%B.

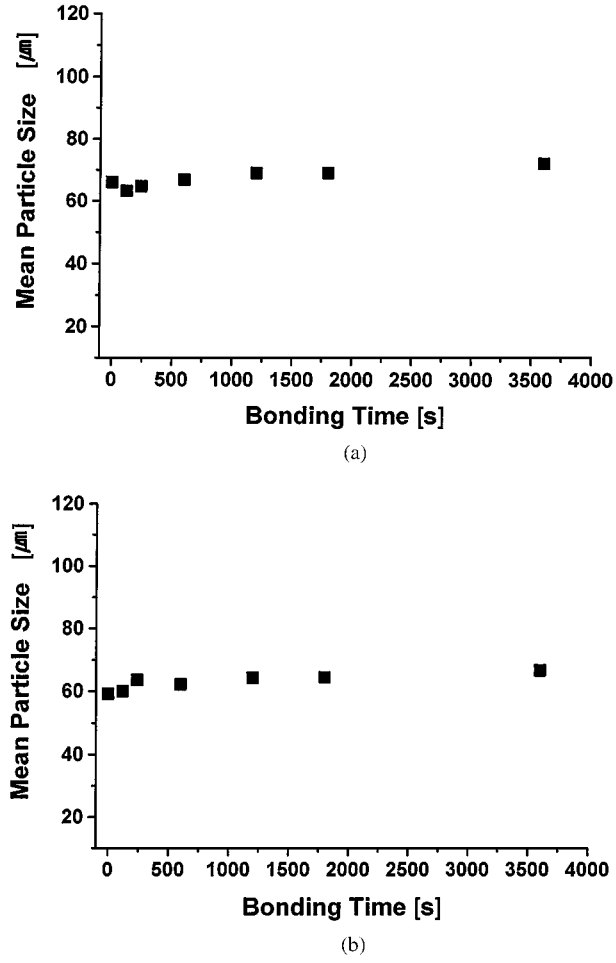

Figure 4 Relationship between mean size of the solid particles in the interlayer and bonding time. The interlayer alloys are (a) Fe-4.5wt%P and (b) Fe-1.16wt%B.

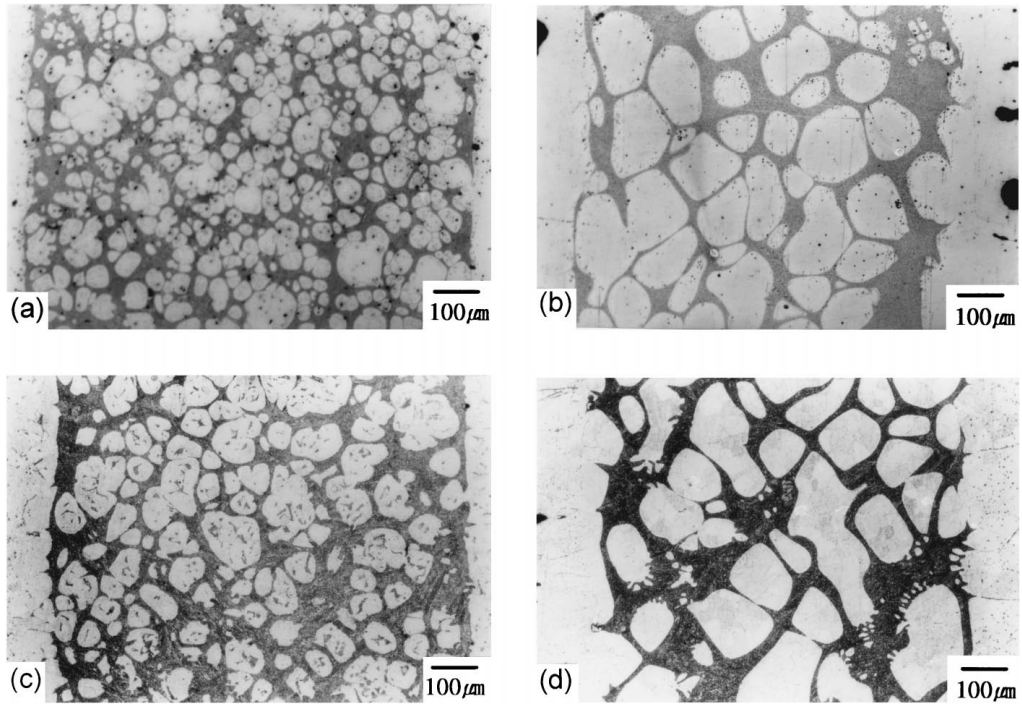

Figure 5 Growth of the solid particles in the interlayer where pure iron particles are allowed to coexist with the liquids of equilibrium composition, which are (a, b) Fe-7.8wt%P at 1473 K and (c, d) Fe-3.2wt%B at 1523 K. (a) 300 s, (c) 600 s, (b, d) 3600 s.

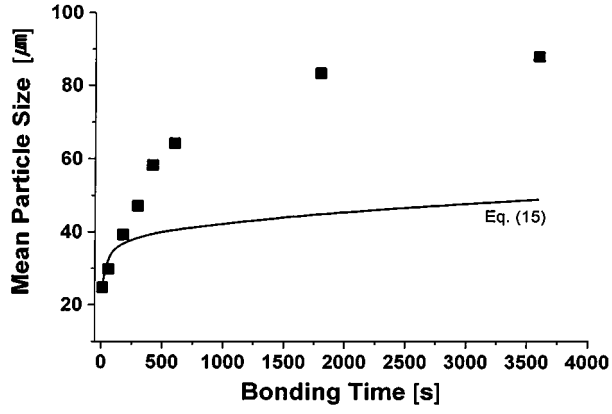

(a)

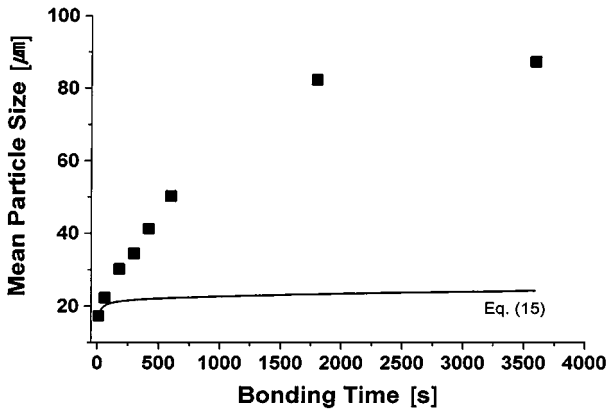

(b)

Figure 6 Plot of mean particle size vs bonding time corresponding to Fig. 5. The liquid compositions are (a) Fe-7.8wt%P and (b) Fe-3.2wt%B.

TABLE I List of physical constants used in calculations

	Fe-4.5wt%P	Fe-1.16wt%B
C_s	0.035 (0.02)[a]	0.01[b] (0.002)[a,b]
C_l	0.132 (0.078)[a]	0.146 (0.032)[a]
V_s[c]	8.05 cm^3/mol	7.42 cm^3/mol
V_l[c]	10.15 cm^3/mol	8.08 cm^3/mol
D[d]	2.2×10^{-8} cm^2/s	1.435×10^{-6} cm^2/s
V_f	0.668	0.623
t_f[c]	9750 s	7524 s

[a]Weight fraction used for Equation 3.
[b]In reference to Section 4.2.
[c]Calculated value.
[d]Solute diffusivity [12].

4. Discussion

4.1. Dependence of the travel distance of the bond interface on time

According to the report of Ikawa *et al.* [4] (later English version by Nakao *et al.* [5]), the travel distance of the bond interface, X, can be expressed by the following equation.

$$X = \frac{2C_s D^{1/2}}{\left(\frac{C_l}{V_l} - \frac{C_s}{V_s}\right) V_s \pi^{1/2}} t^{1/2} \qquad (2)$$

where D is diffusion coefficient of the solute in solid phase, C_l and C_s are equilibrium mole fractions of the solute in the liquid and the solid phase, respectively, and V_l and V_s are molar volumes of the liquid and the solid phase, respectively. When the physical constants listed in Table I are put into Equation 2, the slopes of the X vs. $t^{1/2}$ plot are 0.84 and 1.09 μm $s^{-1/2}$ for Fe-P and Fe-B system, respectively, as shown in Fig. 3.

However, linear regression of the experimental results gives 2.1 and 2.8 for Fe-P and Fe-B system, respectively. The discrepancy between the theoretical value and experimental one is too large to be regarded as an

experimental error. Similar relationship between X and t was also obtained by Lesoult [8]:

$$X = K_3(4Dt)^{1/2} \tag{3}$$

where the constant K_3 is a function of C_0, C_l and C_s. (C_0 is the composition of the base metal and the compositions are in weight fraction.) The values of K_3 are derived [8] and briefly tabulated in reference [6]. By applying the values of C_l and C_s listed in Table I and $C_0 = 0$ K_3 value can be calculated from the list of the derived values, being 0.43 and 0.036 for Fe-P and Fe-B system, respectively. From Equation 3 the slopes are then evaluated to be 1.28 and 0.87 μm s$^{-1/2}$. These are also smaller than those experimentally obtained. The discrepancy between the experimental value and those expected by Equations 2 and 3 is attributed to the contribution of the solid particles distributed in the interlayer. For simplicity it is assumed that the solid particles are of cube having edge length of α and regularly arrayed as shown in Fig. 7a. In region A the movement of the bond interface is diffusion controlled only in β over the distance $\alpha + \beta$. The cubic unit of $(\alpha + \beta)$ is repeated throughout the interlayer. When N is the number of $(\alpha + \beta)$ sector in the moving direction of the bond interface in the half interlayer,

$$\frac{250}{\alpha + \beta} = N \tag{4}$$

Since

$$\frac{\beta}{\alpha} = V_f^{-1/3} - 1 \tag{5}$$

where V_f is volume fraction of the solid particle in the interlayer, Equation 4 is rewritten as

$$\frac{250V_f^{1/3}}{\alpha} = N \tag{6}$$

In region A the interface movement proceeds in such a way as depicted in Fig. 7b. Thus with Equation 6 the slope of the X vs. $t^{1/2}$ plot, m_A, is expressed as follows.

$$m_A = \frac{q}{p} = \frac{\alpha + \left(kt_f^{1/2}/N\right)}{\left(t_f^{1/2}/N\right)} = \frac{250V_f^{1/3}}{t_f^{1/2}} + k \tag{7}$$

where k is the theoretically obtained slope as appeared in Equations 2 or 3, and t_f is the time for complete isothermal solidification. On the other hand, In region B the movement is diffusion controlled all over the distance $\alpha + \beta$, and the slope, m_B, will be simply k. The mean slope, m, is then given as follows.

$$m = \phi_A m_A + \phi_B m_B \tag{8}$$

where ϕ_A and ϕ_B are volume fractions of region A and B, respectively, and expressed by

$$\phi_A = \frac{\alpha^2(\alpha + \beta)}{(\alpha + \beta)^3} = V_f^{2/3} \quad \phi_B = 1 - V_f^{2/3} \tag{9}$$

Then, with Equations 7 to 9

$$m = \frac{250V_f}{t_f^{1/2}} + k \tag{10}$$

By putting t_f and V_f values listed in Table I into Equation 10 and using k value appeared in Equation 2 one can obtain $m = 2.5$ and 2.9 for Fe-P and Fe-B system, respectively. These values give reasonably a good agreement with the slope experimentally obtained. The time for complete solidification, t_f, involved in Equation 10 is important for the calculation of slope. However it is difficult to accurately define t_f because all of the region in the interlayer does not solidify simultaneously. Thus some degree of subjectivity will be involved in determining t_f. t_f can be theoretically obtained from Equation 2 by replacing X with $250(1 - V_f)$, which is the effective distance traversed by diffusion controlled mode. t_f is then 9.75×10^3 s and 7.52×10^3 s for Fe-P and Fe-B system, respectively. The slope obtained above was calculated by using the theoretical t_f. The t_f's are approximately same to the experimentally estimated ones which are 1.08×10^4 s and 7.2×10^3 s for Fe-P and Fe-B system.

It is to be mentioned that the diffusion through the particles attached to the bond interface is not so rapid

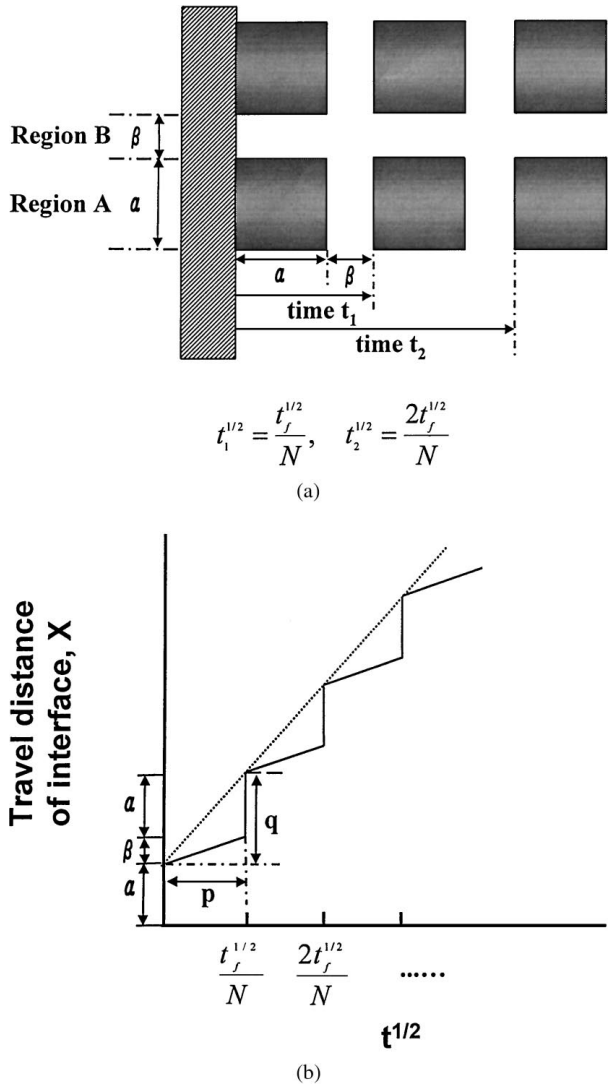

Figure 7 (a) Schematic illustration of solid particles regularly arrayed in such a way that the cubic unit $(\alpha + \beta)$ is repeated throughout the interlayer. (b) Stepwise movement of the bond interface along the region A of Fig. 7a.

as one that would proceed in the absence of the particles, because the concentration of the particle is already saturated, and thus time is needed for building up concentration gradient. However, the retarded diffusion can be compensated by an enhanced diffusion at the concave region (region B in Fig. 7a) where the area of the bond interface through which the solute atoms arrive at the base metal is much larger than in the absence of the particles. Therefore the apparent diffusion flux would be roughly the same in spite of the presence of the particles.

4.2. Solid solubility of B in Fe

Solid solubility of solute atom in the base metal, C_s, is strongly influential to t_f, and in turn, to the slope of X vs. $t^{1/2}$. In the case of Fe-P system solid solubility of P in Fe is determined directly from the phase diagram [9], being 2 wt% (0.035 mole fraction). However, it is not easy to rigorously estimate the solid solubility of B in Fe from the phase diagram, because the phase diagram represents no solid solubility. In principle, if there is no solid solubility of the solute in the base metal, it is impossible for the interlayer to isothermally solidify. Therefore, B should be dissolved in Fe, regardless whether its sink is inside the grain or grain boundary. Best fit of the experimental data for t_f and the slope of X vs. $t^{1/2}$ was obtained when the solid solubility of B in Fe is assumed to be 0.2 wt% (0.01 mole fraction) at the bond temperature, i.e. 1523 K.

4.3. Growth of pure Fe particles in the liquid of equilibrium composition

As shown in Figs 5 and 6, the pure Fe particles undergoes rapid growth when they are allowed to coexist with the liquid of equilibrium composition. It is assumed that Fe particle is spherical and its radius R. At the surface of the Fe particle local equilibrium is maintained such that liquid and solid compositions are C_l and C_s, respectively. While the composition of the liquid is everywhere the same, being C_l, the composition of the solid particle is dependent on the position, diminishing from C_s to zero as the center of the particle is approached. When the particle with radius R grows for dt, it accepts solute atoms from the liquid:

$$J = \left(\frac{C_l}{V_l} - \frac{C_s}{V_s}\right)\frac{d\left(\frac{4}{3}\pi R^3\right)}{dt} = 4\pi R^2\left(\frac{C_l}{V_l} - \frac{C_s}{V_s}\right)\frac{dR}{dt} \tag{11}$$

where J is flux in mole per unit time, and V_l and V_s are molar volumes of the solute in liquid and solid phase, respectively. The accepted atoms should be dissipated inward by solid state diffusion:

$$J = 4\pi R^2 \frac{D}{V_s}\left(\frac{dC}{dr}\right)_{r=R} \tag{12}$$

where C is mole fraction of solute in the solid particle, and r is a distance from the center of the particle. The distribution of the solute in the solid particle will be made under the following boundary condition,

$$C = C_s \quad \text{at } r = R \text{ and } t > 0$$
$$C = 0 \quad \text{at } 0 < r < R \text{ and } t = 0$$

The solution of Fick's 2nd law for spherical coordinate under the above boundary condition is given both graphically and in formula in reference [10]. $(\frac{dC}{dr})_{r=R}$ can then be graphically obtained: (The procedure is described in detail in Appendix.)

$$\left(\frac{dC}{dr}\right)_{r=R} = \frac{0.14 C_s R^{0.6}}{D^{0.8} t^{0.8}} \tag{13}$$

From Equations 11 to 13

$$R^{-0.6}\,dR = \frac{0.14 C_s D^{0.2}}{V_s\left(\frac{C_l}{V_l} - \frac{C_s}{V_s}\right)} t^{-0.8}\,dt \tag{14}$$

Integrating gives

$$R^{0.4} - R_0^{0.4} = \frac{0.28 C_s D^{0.2}}{V_s\left(\frac{C_l}{V_l} - \frac{C_s}{V_s}\right)} t^{0.2} \tag{15}$$

where R_0 is initial radius of the particle. The results of Fig. 6 are redrawn in Fig. 8, where $R^{0.4} - R_0^{0.4}$ is plotted against $t^{0.2}$. Putting appropriate constants into Equation 15 gives the slope 0.165 and 0.06 $\mu m^{0.4}\ s^{-0.2}$ for Fe-P and Fe-B system, respectively. The slopes do not match with the experimental data, and furthermore, $R^{0.4} - R_0^{0.4}$ seems not to be linearly dependent on $t^{0.2}$. Particle growth proceeds more rapidly than expected by Equation 15. This discrepancy can be seen also in Fig. 6. Particle growth in the present situation differs from Ostwald ripening where larger particle grows at the expense of smaller one, thereby the distance between the particles increasing. In the present case any particles, regardless of their size, can grow as long as the solute is provided from the coexisting liquid and the particle is not completely saturated. Therefore it is considered that particle contacting will be unavoidable as growth proceeds, with the result that agglomeration or coalescence simultaneously occurs during the diffusional growth. It always takes place unless the volume fraction of the solid particle is sufficiently low. The particle growth will thus appear as a sum of the contributions provided by both physical particle contacting and an intrinsic diffusional growth. This is depicted in Fig. 8. As revealed in Fig. 5 the Fe particles are in effect very closely distributed, and thus liable to agglomerate or coalesce during the growth process. Contribution by particle contacting will be importantly continued until the stage is attained where small spacings between the particles are almost consumed, and only large spacings survive. At this stage there is little probability to agglomerate or coalesce and the particle growth is completely diffusional until the growing

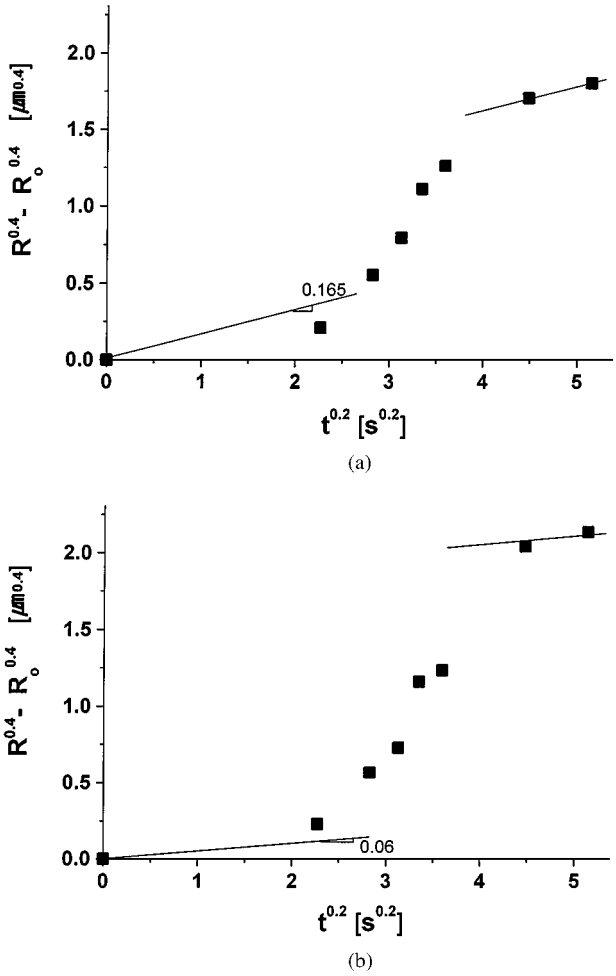

Figure 8 Plot of $R^{0.4} - R_0^{0.4}$ vs. $t^{0.2}$ redrawn from the data of Fig. 6. The solid lines represent growth by Equation 15. The liquid compositions are (a) Fe-7.8wt%P and (b) Fe-3.2wt%B.

surfaces meet others. From the micrographs of Fig. 5 this stage is estimated to be attained after 1500 s.

As described in Appendix, $(\frac{dC}{dr})_{r=R}$ in Equation 13 is not rigorously calculated, but approximately obtained. Therefore, the power of t may not be 0.8. Although error may be involved in determining the exponent, it is reasonable to consider that $(\frac{dC}{dr})_{r=R}$ has a form of $\frac{AR^{2n-1}}{t^n}$ (A, n: constants), and in this case Equation 15 becomes

$$R^{2(1-n)} - R_0^{2(1-n)} = Bt^{1-n}$$

At any combination of n and B similar deviations or even worse will occur because of particle contacting.

What we are concerned about here is the growth of the particle, and it is of no significance how many grains there are in this particle. Therefore, the particle may be single powder or aggregate of the powders, being a unit of solid phase which is surrounded by the equilibrium liquid.

Conclusively, when the pure Fe particles are introduced into the interlayer the bond region will be completely isothermally solidified by both lateral movement of the bond interface and growth of the particles residing inside the interlayer.

5. Summary and conclusion

In the present work the conventional TLP bonding process is slightly modified, with the liquid phase sintered alloy used as interlayer material. At the bonding temperature the interlayer would, then, show a mixed microstructure consisting of the solid particles distributed in the liquid matrix, so that the time needed for isothermal solidification might be reduced. In this case the isothermal solidification will be essentially a combined process where the inward movement of the bond interface proceeds in parallel with the growth of the solid particles (Ostwald ripening). However, only the movement of the bond interface is decisive in isothermal solidification. In spite of coexisting with the liquid phase the solid particles have shown no growth. This is because most of solute atom flux would be directed toward the mating base metals owing to the much larger concentration gradient built up in that direction. The movement of the bond interface was linearly dependent on $t^{1/2}$ with higher slope than that without solid particles in the interlayer. The kinetics could be quantitatively described on the basis of the simplified assumption for the particle array and gave an agreement with the experimental results. When pure Fe particles are coexisting with the liquid of equilibrium composition at the bonding temperature, they are seen to have grown very rapidly. Their growth kinetics was derived similarly to the case of lateral movement of the bond interface, but does not give even a rough approximation. More rapid growth than expected seems to be attributed to particle contacting. With the particles distributed in the interlayer, not only the bonding time is shortened, but also large clearance can be bonded within a reasonable time. In order for the particles to be distributed in the interlayer it will be an effective method to use liquid phase sintered alloy as an interlayer material.

Appendix

If D does not depend on position, Fick's 2nd law for spherical coordinate is

$$\frac{\partial C}{\partial t} = D\left(\frac{\partial^2 C}{\partial r^2} + \frac{2}{r}\frac{\partial C}{\partial r}\right) \qquad \text{(A1)}$$

When the boundary condition is given by

$$C = C_s \quad \text{at } r = R \text{ and } t > 0$$
$$C = 0 \quad \text{at } 0 < r < R \text{ and } t = 0$$

the solution of Equation A1 for small times is expressed as [11]

$$\frac{C}{C_s} = \frac{R}{r}\sum_{n=0}^{\infty}\left\{\text{erfc}\frac{(2n+1)R - r}{2(Dt)^{1/2}} - \text{erfc}\frac{(2n+1)R + r}{2(Dt)^{1/2}}\right\} \qquad \text{(A2)}$$

Plot of (C/C_s) in terms of r/R for different values of Dt/R^2 is reproduced from reference [10] in Fig. A1.

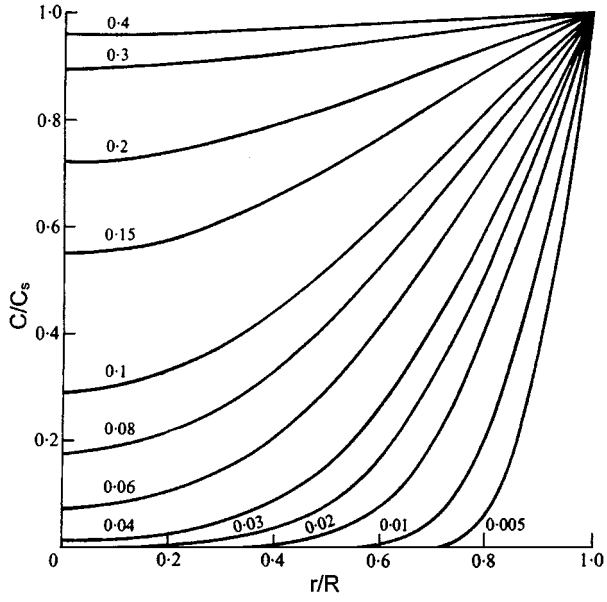

Figure A1 Plot of C/C_s vs. r/R for various values of Dt/R^2 [10].

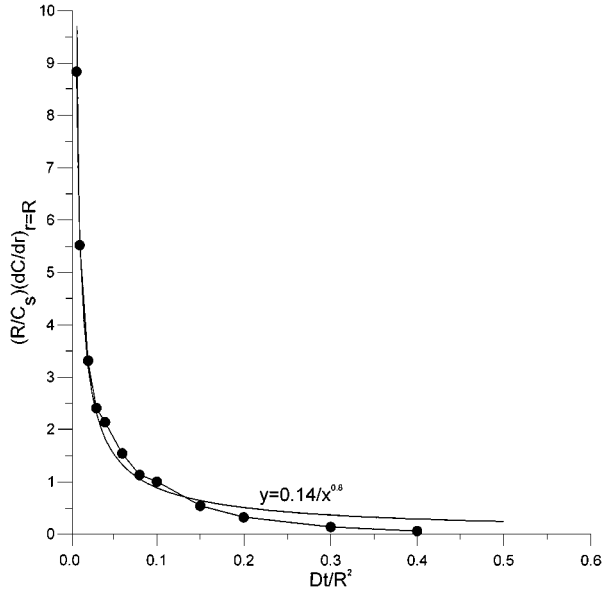

Figure A2 The data points represent the slopes of the tangent at $r/R = 1$ for various Dt/R^2 which are graphically obtained from Fig. A1. The point trace can be reasonably well expressed by Equation A3.

The slope of the curves at $r/R = 1$ was graphically determined by drawing the tangent and is plotted against Dt/R^2 in Fig. A2. If it is assumed that the curve has a form of $y = E/x^n$ (E, n: constant) in order to simplify the calculations following, a reasonably good fit is made when $E = 0.14$ and $n = 0.8$, as shown in Figure A2. Therefore

$$\frac{R}{C_s}\left(\frac{dC}{dr}\right)_{r=R} = \frac{0.14}{(Dt/R^2)^{0.8}} \qquad \text{(A3)}$$

or

$$\left(\frac{dC}{dr}\right)_{r=R} = \frac{0.14 C_s R^{0.6}}{D^{0.8} t^{0.8}} \qquad (13)$$

Acknowledgement

This study was financially supported by Korea Research Foundation under grant No. 1997-001- E00630. Support from the Korea Science and Engineering Foundation (KOSEF), through the Center for Interface Science and Engineering of Materials, KAIST, is also gratefully acknowledged.

References

1. D. S. DUVALL, W. A. OWCZARSKI and D. F. PAULONIS, *Welding Journal* **204** (1974) 203.
2. Y. NAKAO, K. NISHMOTO, K. SHINIZAKI, C. Y. KANG and H. SHIGETA, *Trans. Jpn. Weld. Soc.* **23**(2) (1992) 82.
3. E. E. UNDERWOOD, "Quantitative Stereology" (Addison-Wesley Publ., Reading, 1970) p. 80.
4. H. IKAWA, Y. NAKAO and T. ISAI, *J. Jpn. Weld. Soc.* **47** (1978) 440.
5. Y. NAKAO, K. NISHMOTO, K. SHINOZAKI and C. Y. KANG, *Trans. Jpn. Weld. Soc.* **20**(1) (1989) 60.
6. I. TUAH-POKU, M. DOLLAR and T. B. MASSALSKI, *Metall. Trans.* **19A** (1988) 675.
7. J. W. MARTIN and R. D. DOHERTY, "Stability of Microstructure in Metallic Systems" (Cambridge University Press, London, 1976) p. 182.
8. G. LESOULT, cited in reference 6.
9. T. B. MASSALSKI (ed.), "Binary Alloy Phase Diagrams" (ASM, Metals Park, 1986).
10. J. CRANK, "The Mathmatics of Diffusion" (Clarendon Press, Oxford, 1975) p. 91.
11. H. S. CARSLAW and J. C. JAEGER, cited in reference 10.
12. "Kinzoku Data Book" (Japan Inst. Metals, Maruzen, Tokyo, 1993) p. 22.

Received 18 February
and accepted 19 August 1999